



## Study of Ni(II) removal by olive tree pruning and pine cone shell by experimental design methodology

Ana Isabel Almendros Molina, Alicia Ronda Gálvez\*, María Ángeles Martín-Lara, Gabriel Blázquez García, Mónica Calero de Hoces

Department of Chemical Engineering, University of Granada, 18071 Granada, Spain, Tel. +34 958 243315; Fax: +34 958 248992; emails: [anaalmendros@correo.ugr.es](mailto:anaalmendros@correo.ugr.es) (A.I. Almendros Molina), [alirg@ugr.es](mailto:alirg@ugr.es) (A. Ronda Gálvez), Tel. +34 958 240445; Fax: +34 958 248992; email: [marianml@ugr.es](mailto:marianml@ugr.es) (M.Á. Martín-Lara), Tel. +34 958 243315; Fax: +34 958 248992; emails: [gblazque@ugr.es](mailto:gblazque@ugr.es) (G.B. García), [mcalero@ugr.es](mailto:mcalero@ugr.es) (M.C. de Hoces)

Received 14 May 2015; Accepted 30 June 2015

### ABSTRACT

The overall objective of this study is to model and optimize the elimination of nickel ions from aqueous solutions by pine cone shell and olive tree pruning as biosorbents. A  $3^3$  full factorial design was employed for experimental design and analysis of the results. The flow rate (4–8 mL/min), the mass of biosorbent (5–15 g), and the initial Ni(II) concentration (10–100 ppm) were the critical variables of the removal optimized. The results have shown that initial concentration of Ni(II) is the most influential factor in biosorption capacity as much as in total nickel removal. The optimum flow rate, mass of biosorbent, and initial concentration of Ni(II) to obtain the maximum total nickel removal coincided with both biosorbents and were found to be 6 mL/min, 15 g, and 10 ppm. Meanwhile, to maximize the biosorption capacity, the optimum flow rate, mass of biosorbent, and initial concentration of Ni(II), were 8 mL/min, 5 g, and 100 ppm for olive tree pruning and 6 mL/min, 15 g, and 100 ppm for pine cone shell. The experimental breakthrough curves obtained under optimum conditions were modeled using Bohart–Adams, Thomas, Yoon–Nelson, and Dose-Response models. The last one is the model that best reproduced the total breakthrough curves.

*Keywords:* Biosorption; Nickel; Pine cone shell; Olive tree pruning

### 1. Introduction

Contamination of aqueous environment by heavy metals has been a major cause of concern over the last few decades. Heavy metals are non-biodegradable and tend to accumulate in living organisms, thus becoming concentrated throughout the food chain [1]. In soil and water, heavy metals are introduced from the waste discharge of the industrial manufacture, such as

pesticides, batteries, alloys, electroplated material, textile dyes, steel [2]. There are an increasing number of applications with nickel us steel, rechargeable batteries of NiCd and NiMH, etc., due to its good properties against corrosion, impact, and high temperatures [3]. The average concentration of nickel in drinking water is between 2 and 4.3 ppb [4]. However, near the industries that process or use Ni(II), the levels could be higher, and it is necessary to decrease this value until acceptable levels.

\*Corresponding author.

Conventional separation techniques, including chemical precipitation, membrane separation, filtration, ion exchange, electrochemical methods, etc. have been developed to respond to this challenge [5]. However, these methods are limited in practice due to the drawbacks, such as formation of undesirable metallic by-products, rigorous conditions, or expensive cost [6].

Biosorption technology, one of the emerging methods for metal removal, has been regarded as a cheaper and more effective alternative [7]. Biosorbents for the removal of heavy metal ions mainly come under the following categories: bacteria, fungi, algae, industrial waste, agricultural wastes, and other polysaccharide materials [8]. Many agricultural wastes have been studied to remove nickel from wastewater as grapefruit peel, peanut hull, barley straw, sugarcane, rice bran, baker's yeast, wheat, pomace of olive oil factory, palm seed, sugar beet pulp, rice husk, coir pith, orange peel, cassava peel, and cashew nut peel [9–20]. In this work, the use of pine cone shell (PCS) and olive tree pruning (OTP) as biosorbents to remove nickel from artificial waste waters was studied.

The presence of chemical compounds such as holo-cellulose,  $\alpha$ -cellulose and lignin provides acidic functional groups which accounts for the metal capacity of both biosorbents [21–23]. Two materials are wastes of agro-industrial activity and they are highly abundant in nature. Besides, they present an advantage that the small contact period required to remove a large amount of metal ion from solution is short. The literature search revealed that equilibrium of heavy metal uptake was reached in the first 7 min for Nickel(II) onto pine cone powder [24]. Shorter contact time means higher metal removal rates within short times.

The novelty of this research is that it made a deep study of the biosorption continuous process to remove nickel from wastewater because there is barely any literature about the breakthrough curves of this metal.

Moreover, although multivariate statistical techniques have been widely studied by many researchers for the optimization of biosorption process in batch mode [25–27], there is no study in the literature on response surface modeling of nickel removal from aqueous solution by PCS and OTP using an experimental design technique.

The classical method of experimental optimization involves changing one variable at a time, keeping the others constant. In addition, it is not practical to carry out experiments with every possible factorial combination of the test variables because of the large number of experiments required. Thus, a  $3^3$  full factorial design was used in this study to establish how initial concentration of Ni(II), mass of biosorbent, and flow rate interacted in the removal of Ni(II), besides to

obtain mathematical models that show the influence of each variable and their interactions.

## 2. Materials and methods

### 2.1. Biomass

OTP was obtained from olive plantation located in Vilches, province of Jaen (Spain). The solid was milled in an analytical mill (IKA MF-10) and <1.000 mm fraction was chosen for the characterization and biosorption tests.

PCS was provided by Carsan Biocombustibles S.L. Factory from Granada (Spain). The solid was milled in an analytical mill (IKA MF-10) and the <1.000 mm fraction was chosen for the characterization and biosorption tests.

A complete characterization of solids has been made in previous works [23].

### 2.2. Preparation of nickel solutions

A series of stock solutions of 10, 50, and 100 mg/L Ni(II) were prepared by dissolving the desired amount of  $\text{Ni}(\text{NO}_3)_2 \cdot 6\text{H}_2\text{O}$  (riches 98%) in 10,000 mL of distilled water. Solutions of different concentrations were prepared by the dilution of appropriate quantities of Ni(II).

### 2.3. Continuous system

Continuous flow sorption experiments were conducted in a glass column with an internal diameter of 1.5 cm and length of 23 cm. A known quantity of the biosorbent was packed in the column to yield the corresponding bed height of the biosorbent. The bed porosity was 0.673 and 0.702 and the bulb density was equal to 0.472 and 0.422 g/cm<sup>3</sup> for PCS and OTP, respectively. The bed of the biosorbent was supported between two small layers of cotton wool to prevent the biosorbent from floating. To enable a uniform inlet flow of solution into the column, glass beads of 5 mm diameter were placed into the column. The nickel solution having the chosen initial concentration was then pumped through the column at desired volumetric flow rate with the help of a peristaltic pump (Dinko model D21 V) in an up-flow mode at constant temperature (maintained at 25°C with a thermostatic bath). Samples were collected from the outlet of the column at a time interval of 10 min during an operation time of 250 min and were analyzed by a 3,100 Perkin–Elmer atomic absorption spectrophotometer to obtain the nickel concentration of samples.

The experimental breakthrough curves were obtained by measuring the metal concentration in the

effluent samples collected. When the volume of the fluid begins to flow through the column, the mass-transfer zone varies from 0% of the inlet concentration, corresponding to the solute-free biosorbent, to 100% of the inlet concentration, corresponding to the total saturation [28]. From a practical point of view, in this study, the saturation time,  $t_s$ , is established when the concentration of the effluent is 90% of the inlet concentration; and the service or breakthrough time,  $t_r$ , is established when the metal concentration in the effluent reaches a value between 1 and 2 mg/L. The breakthrough curve is usually expressed in terms of a normalized concentration, defined as the ratio of effluent metal concentration to inlet metal concentration ( $C/C_i$ ) vs. time or volume of the effluent.

Analysis of column data was obtained and evaluated with the help of following equations:

- (1) Volume of the effluent ( $V_{ef}$ ) in mL:

$$V_{ef} = Q t_{total} \quad (1)$$

$Q$  = volumetric flow rate in mL/min;

$t_{total}$  = total flow time in min.

- (2) Total mass of metal biosorbed (the area under the breakthrough curve) ( $q_{total}$ ) in mg:

$$q_{total} = Q/1,000 \int_{t=0}^{t=t_{total}} C_R dt \quad (2)$$

$C_R$  = concentration of metal removal in mg/L.

- (3) Total amount of metal ions sent to the column ( $m_{total}$ ) in mg:

$$m_{total} = \frac{C_i Q t}{1,000} \quad (3)$$

- (4) Total metal removal (% $R$ ) in %:

$$\%R = \frac{q_{total}}{m_{total}} \times 100 \quad (4)$$

- (5) The amount of metal biosorbed at equilibrium or biosorption capacity ( $q_e$ ) in mg of sorbated metal/g of biosorbent:

$$q_e = \frac{q_{total}}{m} \quad (5)$$

$m$  = mass of biosorbent in g.

- (6) The equilibrium metal concentration ( $C_e$ ) in mg/L:

$$C_e = \frac{m_{total} - q_{total}}{V_{ef}} \times 1000 \quad (6)$$

#### 2.4. Modeling by full factorial design and optimization of operational variables

The factorial design describes which factor shows more impact on response and the relationships between all factors and response [29]. In this work, volumetric flow rate, initial Ni(II) concentration, and biosorbent dose were taken as independent variables while the other variables like the particle size (<1 mm), temperature (25°C), and total flow time (250 min) were kept constants. Responses examined were the biosorption capacity and Nickel removal percentage. Three replicates of 3<sup>3</sup> FFD having 27 experiments (with one replicate) were studied. Then 27 (3<sup>3</sup>) measurements are required to perform a factorial design analysis. The three factors and three levels for OTP and PCS are shown in Table 1.

#### 2.5. Modeling data

Results with the best operational conditions obtained from experimental design were modeled to estimate the kinetic coefficients. Various simple mathematical models, such as Adams–Bohart, Thomas, Yoon–Nelson, and Dose-response models have been developed to predict the dynamic behavior of the column and allow some kinetic coefficients to be estimated. These models have been widely used by several authors to model the biosorption process. The necessary equations for each model are presented below. The full development for them can be seen in previous works [28,30,31].

Table 1  
Values and levels of operating parameters for OTP and PCS

Factors	Levels		
	-1	0	1
$X_1$ : volumetric flow rate, mL/min	4	6	8
$X_2$ : mass of biosorbent, g	5	10	15
$X_3$ : initial nickel concentration, mg/L	10	50	100

(7) Adams–Bohart model:

$$\frac{C}{C_i} = e^{k_{AB} C_i t} - \frac{k_{AB} N_0 Z}{v} \quad (7)$$

$k_{AB}$  = kinetics constant in L/mg min;

$N_0$  = maximum volumetric sorption capacity in mg/L;

$C$  = solute concentration in the liquid phase in mg/L;

$C_i$  = inlet metal concentration in the solution in mg/L;

$v$  = linear flow rate in cm/min and  $Z$  is the bed depth of the column in cm.

This model is going to be applied to describe the initial part of the breakthrough curve, i.e. for  $C$  values lower than  $0.15 C_i$ .

(8) Thomas model:

$$\frac{C}{C_i} = \frac{1}{1 + \exp\left(\frac{k_{Th}}{Q}(q_0 m - C_i V_{ef})\right)} \quad (8)$$

$k_{Th}$  = the Thomas rate constant in mL/min mg;

$q_0$  = maximum concentration of the solute in the solid phase in mg/g.

(9) Yoon and Nelson model:

$$\frac{C_i}{C} = \frac{1}{1 + e^{k_{YN}(\tau - t)}} \quad (9)$$

$k_{YN}$  = the Yoon and Nelson's proportionality constant in  $\text{min}^{-1}$ ;

$\tau$  = time required for retaining 50% of the initial adsorbate in min.

(10) Dose-response model:

$$\frac{C}{C_i} = 1 - \frac{1}{1 + \left(\frac{C_i V_{ef}}{q_0 m}\right)^a} \quad (10)$$

$a$  = the constant of the Dose-response model.

### 3. Results and discussions

#### 3.1. Biosorption of Ni(II)

In this section, the effect of the main factors, that affect the biosorption process, is studied and a full

factorial design is applied to know which factor or pair of them has more influence on it.

##### 3.1.1. Study of the effects of factors

**3.1.1.1. Effect of feed flow rate.** First, the effect of feed flow rate has been analyzed. For that, other parameters have been kept constant according to the previous studies performed in continuous system [32] and data from literature: initial concentration of Ni(II), 100 mg/L; pH 6; time of contact, 250 min; and mass of OTP or PCS, 5 g (equivalent to 7 cm of the height of bed column for OTP and 6 cm for PCS). For all experiments,  $t = 0$  has been assigned to the time in the exit of the column, with the objective that all of them have the same reference point.

The breakthrough curves at three flow rates (4, 6 and 8 mL/min) have been illustrated in Fig. 1.

The removal of Ni(II) increases while the flow rate decreases, reaching the saturation of the column in the three cases with both biosorbents. Also, the breakthrough time,  $t_r$ , increases when the flow rate decreases. Since the ratio  $C/C_i$  is upper 0.8, using OTP as biosorbent, there are not almost differences between the behavior with the two highest flow rates (6 and 8 mL/min) meanwhile the breakthrough curve for the lowest flow rate is separated of them. In the right graphic, for the PCS since the same point, the behavior with the three flow rates is practically the same. In addition, figures show that PCS is saturated earlier than OTP in the same conditions of the experiment.

This behavior is due to that at a low rate of influence, metal ions had more time to contact the biosorbent, that resulted in a higher removal of metal ions in column. While increasing the flow rate, the results indicated that the adsorption capacity would reach the equilibrium value faster, which may cause a negative effect on the mass transferring efficiency of metal ions. Similar results were obtained for other authors in the biosorption of metal onto different materials [33–35]. Taking into account this effect, it is possible to choose an appropriate flow rate in order to make the process time efficient.

**3.1.1.2. Effect of bed height.** The removal of metals in a packed bed column depends on the amount of biosorbent used (or bed height of column), among other factors. Therefore, the effect of mass of biosorbent on biosorption of Ni(II) has been studied. For that, experiments with three amounts of biosorbents equivalent to three bed heights are performed. There have been used 5, 10, and 15 g of OTP (equivalent to 7, 14.5, and 18 cm respectively) and 5, 10, and 15 g of PCS (equivalent to 6, 12, and 18 cm respectively). According to the

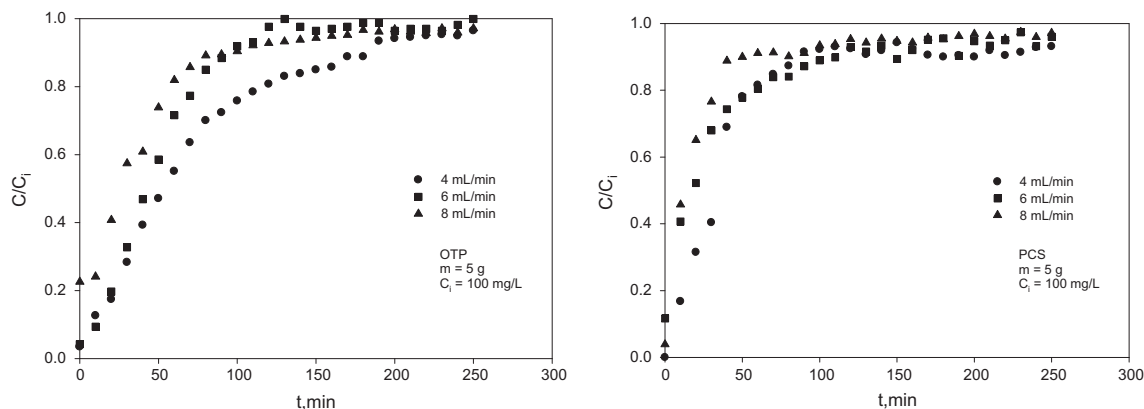


Fig. 1. The effect of feed flow rate on biosorption of Ni(II) onto OTP and PCS.

previous results, flow rate of 4 mL/min and initial concentration of Ni(II), 100 mg/L, pH 6, time of contact 250 min, have been chosen. Results are shown in Fig. 2.

Fig. 2 shows that an increase in bed height increases the nickel removal, and it is better for PCS than for OTP. As the bed height increases, Ni(II) had more time to contact the biosorbents that resulted in higher removal efficiency of Ni(II) ions in column. Besides, the time required for attaining the breakthrough or saturation increased with an increase in bed height in the case of both biosorbents. Similarly, volume was treated till breakthrough and saturation increased with an increase in bed height. It is due to that, when the column has greater bed height, it contains a larger amount of biosorbent and thus it provides a greater number of sites for the binding of metal ions. However, when the column has shorter bed height, it is saturated quickly due to lesser availability of sorbent and hence the metal binding sites.

Similar observations were made by several authors by studying the biosorption of different metals in a packed bed column [36–39]. The slope of breakthrough curve decreased with an increase in bed height. The value of the slope of the breakthrough curve reflects the speed to achieve the saturation of the column and consequently, a broadened mass transfer zone. Besides, the slope of breakthrough curve to remove Ni(II) by PCS was lower and thus, saturation of the column was slower using this biosorbent than OTP.

**3.1.1.3. Effect of initial concentration.** The effect of initial concentration of Ni(II) has been studied. For that, experiments are performed, keeping the other variables constants (flow rate, bed height, pH and time). According to the previous studies, flow rate of 4 mL/min, biosorbent mass of 15 g, pH 6, and time of contact 250 min, have been chosen. Results are shown in Fig. 3.

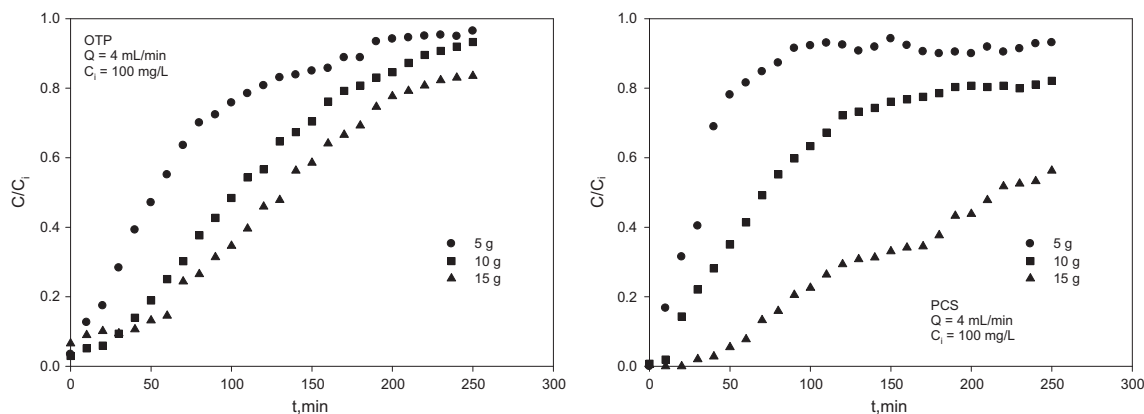


Fig. 2. The effect of mass biosorbent on biosorption of Ni(II) onto OTP and PCS.

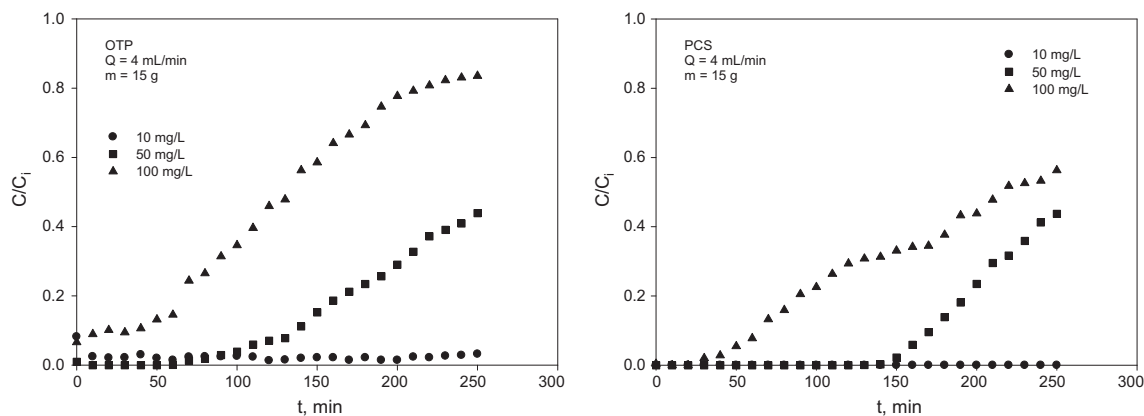


Fig. 3. The effect of initial concentration of nickel on biosorption of Ni(II) onto OTP and PCS.

It is observed that, when initial concentration of nickel is increased, the breakthrough time is less, and the saturation of column will be reached more quickly. Also, the figure shows that the saturation process is slower for PCS than for OTP as biosorbent.

The breakthrough time decreases by increasing the initial concentration of Ni(II), but it is only obtained in a test with the highest initial concentration by using OTP as biosorbent. Consequently, the percentage of Ni(II) removal until saturation of the column was only reached in this experiment. Therefore, to obtain this value in the other cases, more operational time would be necessary and the percentage of metal removed, until the saturation, would be higher. The biosorption capacity was higher using PCS at the same inlet concentration. However, this value for the same waste increased as the inlet Ni(II) concentration increased. It is due to that, at higher metal concentration, sorption of Ni(II) ions by biosorbents is faster than that at a lower concentration, thus resulting in quick attainment of breakthrough and saturation of the column. Finally, it was also observed that the slope of breakthrough curves for both biosorbents increased with an increasing influent metal concentration. As the slope of breakthrough curve is a measure of the efficiency of column to achieve the saturation, one more time, it indicates the faster saturation of the column when inlet Ni(II) concentration increased. Similar to this observation, several authors also found a steeper breakthrough curve at higher concentrations of studied metal in a packed bed column [37,38].

### 3.1.2. Modeling by full factorial design and optimization using the obtained functions

Once studied, that all proposed factors affect the process of biosorption of nickel, a factorial design was

applied to obtain the optimal conditions. The factorial design was performed for two biosorbents.

The natural parameters and coded values of factors (feed flow rate, mass of biosorbent, and initial concentration of Ni(II)) with the values of two studied responses (biosorption capacity,  $Y_1$ , and percentage of nickel removal,  $Y_2$ ) are shown in Table 2.

From these experimental results, the following analysis is carried out:

**3.1.2.1. Pareto plot.** The Pareto analysis indicates the extent of the influence of each variable on the response factor, and it is determined by calculating the percentage effect of each term on response [40]. Results obtained for the two studied responses and for each variable from Pareto analysis are shown in Fig. 4.

In Pareto plot, the vertical line indicates the minimum statistically significant effect of magnitude and the horizontal column lengths are proportional to the significant degree for each effect. The negative factors indicate an unfavorable or antagonistic effect on the response, whereas the positive factors indicate a favorable or synergistic effect on this [41].

Fig. 4 includes the importance of term C in the two responses (both linear and quadratic), indicating the high effect of the initial concentration of Ni(II) in the biosorption process. The initial nickel concentration (C) has a positive effect on biosorption capacity and had a negative effect on %R, the percentage removal, as it was expected, according to the respective definition equations and according to the breakthrough curves obtained and shown in Fig. 3. Note that the influence of initial concentration of nickel is higher for OTP than for PCS because PCS can absorb more nickel with higher initial concentrations than OTP.

Table 2  
FFD Matrix for OTP and PCS. Natural and coded values of parameters

Runs	Coded values			Natural values			Responses			
	X <sub>1</sub>	X <sub>2</sub>	X <sub>3</sub>	Volumetric flow rate (mL/min)	Mass of biosorbent (g)	Initial Ni(II) concentration (mg/L)	OTP		PCS	
							Y <sub>1</sub> (mg/g)	Y <sub>2</sub> (%)	Y <sub>1</sub> (mg/g)	Y <sub>2</sub> (%)
1	-1	-1	-1	4	5	10	1.561	83.87	1.914	94.05
2	-1	-1	0	4	5	50	5.684	55.08	2.716	26.31
3	-1	-1	1	4	5	100	6.039	30.10	4.109	20.48
4	-1	0	-1	4	10	10	1.117	99.88	1.016	99.84
5	-1	0	0	4	10	50	4.005	77.62	3.049	59.09
6	-1	0	1	4	10	100	4.724	47.09	4.139	41.26
7	-1	1	-1	4	15	10	0.796	97.77	0.717	100
8	-1	1	0	4	15	50	3.804	87.28	3.313	92.03
9	-1	1	1	4	15	100	4.442	55.35	5.382	74.42
10	0	-1	-1	6	5	10	2.601	85.22	2.877	89.19
11	0	-1	0	6	5	50	7.454	48.16	4.376	27.02
12	0	-1	1	6	5	100	6.316	20.98	5.419	16.65
13	0	0	-1	6	10	10	1.360	99.85	1.604	99.45
14	0	0	0	6	10	50	5.214	64.49	5.182	63.97
15	0	0	1	6	10	100	6.958	46.24	6.906	42.44
16	0	1	-1	6	15	10	1.113	99.06	1.063	98.88
17	0	1	0	6	15	50	4.763	73.64	4.594	85.08
18	0	1	1	6	15	100	7.077	58.79	7.505	69.18
19	1	-1	-1	8	5	10	2.627	64.55	2.821	69.29
20	1	-1	0	8	5	50	7.267	35.21	5.765	27.93
21	1	-1	1	8	5	100	6.885	17.16	4.785	11.92
22	1	0	-1	8	10	10	1.890	92.89	2.113	98.28
23	1	0	0	8	10	50	5.546	53.74	5.205	48.20
24	1	0	1	8	10	100	8.170	40.72	6.932	31.95
25	1	1	-1	8	15	10	1.580	97.02	1.321	97.34
26	1	1	0	8	15	50	4.917	59.56	3.327	48.35
27	1	1	1	8	15	100	8.376	52.19	4.803	35.91

Similar effects were observed for the volumetric flow rate in two responses. Flow rate had a positive effect on biosorption capacity and had a negative effect on % removal, as well as its effect was more significant for OTP than for PCS. Meanwhile, the mass of biosorbent had a negative effect on biosorption capacity and had a positive effect on % removal. Moreover, its effect is again more significant for OTP than for PCS.

However, the quadratic terms had a different contribution, whereas the quadratic term of CC and BC has a high effect on two responses, the other ones have a very low contribution, even below vertical line. In most cases, the interaction between volumetric flow rate and initial concentration of metal, as well as the volumetric flow rate and mass of biosorbent, has no significant effect on the nickel biosorption process.

So, on examining Fig. 4, it can be observed that all the linear terms had a significant effect on two

responses, and for that in the biosorption process, except the mass of biosorbent using PCS which is not statistically significant for the biosorption capacity.

*3.1.2.2. The main effect plot.* The main effect plots are used to compare the changes in the mean levels to see which factors influence the response more. A main effect is present when different levels of a factor affect the response differently. A line is drawn to connect the points for each factor and a reference line is also drawn at the overall mean. When the line is horizontal (parallel to the  $x$ -axis), there is no main effect present. Each level of the factor affects the response in the same way and the mean response is the same across all factor levels. When the line is not horizontal (parallel to the  $x$ -axis), there is a main effect present. Different levels of the factor affect the response differently. The greater the difference in the vertical position of

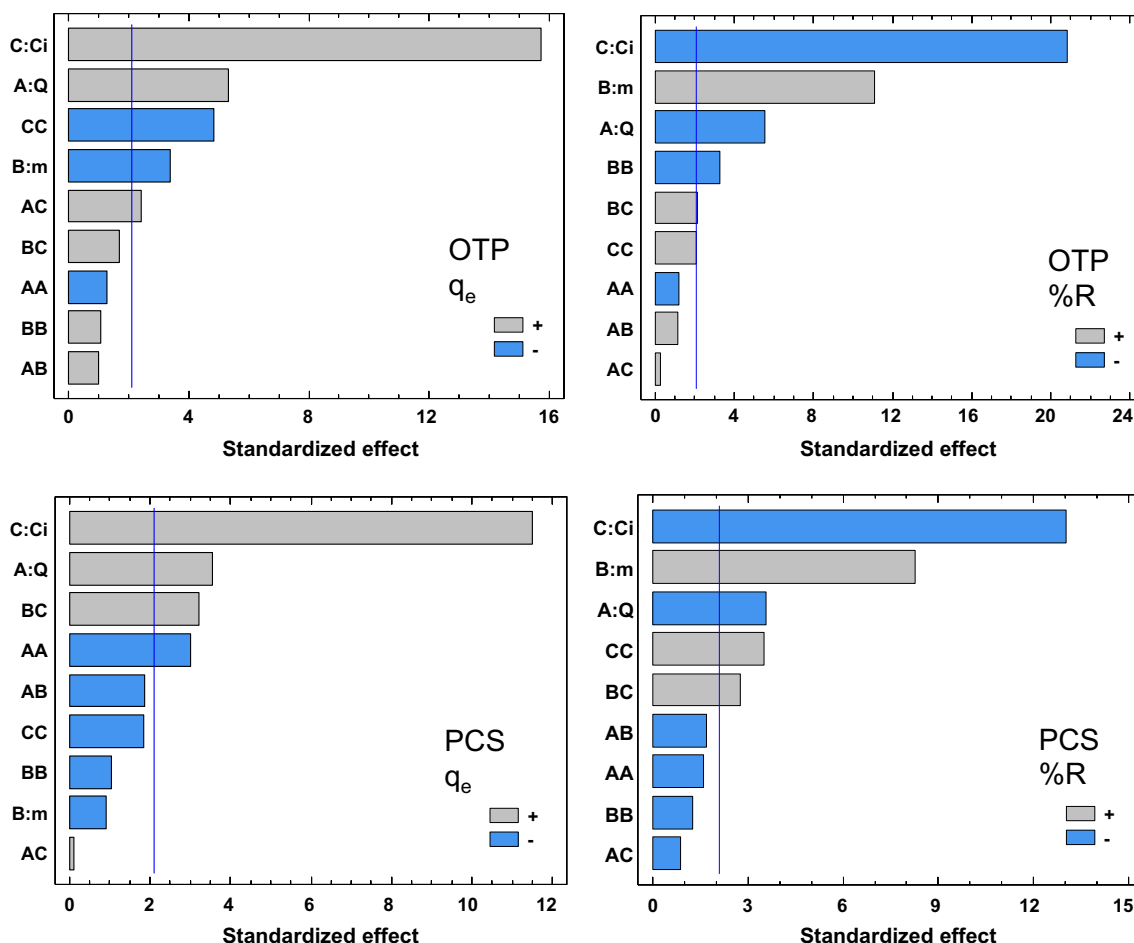


Fig. 4. Standardized Pareto plot for the biosorption capacity (left) and the percentage of nickel removal (right) with OTP and PCS as biosorbents.

the plotted points (the more the line is not parallel to the  $x$ -axis), the greater is the magnitude of the main effect [42].

The studied parameters were the same as above and the main-effects plots are given for each biosorbent in Fig. 5.

It is observed that three factors affect the response differently, being the initial Ni(II) concentration ( $C$ ), the factor which affects more (it is also shown in Pareto plots). The biosorption capacity shows a clear trend to increase with an increase in the initial Ni(II) concentration. It is common for both biosorbents. However, other parameters were not found a clear trend, keeping more or less constant with increase of parameters, as the mass of biosorbent ( $B$ ). Results showed that in the case of PCS, this factor does not affect the biosorption capacity (also in Pareto plots). It can be due to from a value of bed height when it is used PCS the behavior of the column is very similar

and accordingly results of the biosorption capacity value. In Fig. 2, it can be observed that differences in the breakthrough curve were higher between 10 and 15 g of the PCS, whereas these differences decrease between the curves using 5 and 10 g. Besides, analyzing the results from Table 2, a clear trend was not observed in the bed height. So, for an inlet Ni(II) concentration of 50 mg/L, it is observed that biosorption capacity of PCS at flow rate of 4 mL/min was 2.716, 3.049, and 3.313 mg/g for a bed height of 5, 10, and 15, respectively (increasing trend), whereas at a flow rate of 6 mL/min was 4.376, 5.182, and 4.594 mg/g for a bed height of 5, 10, and 15, respectively, (not clear trend) and at flow rate of 8 mL/min was 5.765, 5.205, and 3.327 mg/g for a bed height of 5, 10, and 15, respectively (decreasing trend). Thus, it can be concluded that the biosorption process is very complex and involves many factors. And depending on how other variables affect the process, the parameters can

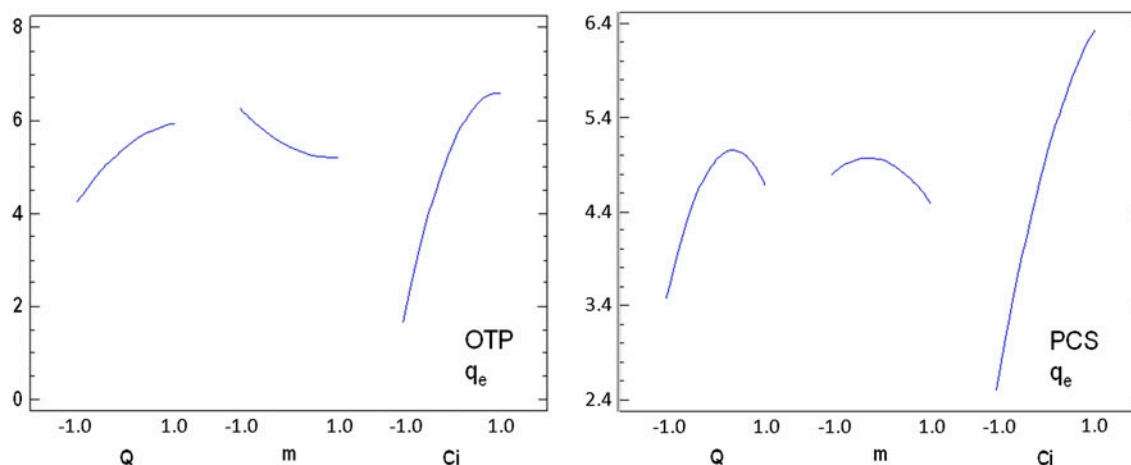


Fig. 5. Main effects for  $q_e$  for the nickel removal with OTP and PCS.

positively or negatively influence the output response variable. For this, the parameters don't have the same effect on the response variable.

**3.1.2.3. Regression analysis.** Data obtained were fitted on a second-order regression equation in the following form:

$$Y = a_0 + a_1 \cdot A + a_2 \cdot B + a_3 \cdot C + a_4 \cdot A^2 + a_5 \cdot A \cdot B + a_6 \cdot A \cdot C + a_7 \cdot B^2 + a_8 \cdot B \cdot C + a_9 \cdot C^2 \quad (11)$$

where  $Y$  is the studied response (nickel biosorption capacity or removal percentage),  $A$ ,  $B$ , and  $C$  studied factors,  $a_0$  the global mean and  $a_i$  is the regression coefficient. The fitted equations for two responses are obtained by substituting the coefficients  $a_i$  in Eq. (11) by the corresponding values from Tables 3 and 4.

Values of standard deviations,  $R^2$  are also given in Tables 3 and 4. High values of  $R^2$  have been observed (higher 91% in all studied cases). They indicated a good fitting of models and high relation between the observed and predicted values of responses. Olmez [43] suggested that the correlation coefficient ( $R^2$ ) should be at least 80% for a good fit of a model. So, the obtained  $R^2$  values showed that the regression models explained well the relation between factors and studied responses by the corresponding second-order equations. On the other hand, values of  $R^2$  indicate that the model with the best results is the best suited for % nickel removal using OTP as biosorbent, as, it presents the highest value for  $R^2$  for four studied responses.

Graphs of the predicted responses values vs. the experimental response values for  $q_e$  and %R, for both

biosorbents, are shown in Figs. 6 and 7, respectively. These figures show that the developed models were adequate due to their good fitting.

**3.1.2.4. Analysis of variance (ANOVA).** An ANOVA was performed to study the significance of the model. Thus, an ANOVA was conducted to obtain the sum of squares (SS), degrees of freedom (Df), mean squares (MS), f-ratio (F-R), and  $p$ -values ( $p$ -V) by fitting the second-order polynomial equation from the experimental data. The results of the coefficients of the model and the ANOVA are shown in Table 5.

It was observed from Table 5 that, the coefficients for the main effects were highly significant for two biosorbents ( $p = 0.000$ ), while for the mass of PCS, the effect  $B$  was not significant ( $p = 0.3716$ ). It is well known that for the larger magnitude of F-R and smaller  $p$ -value, more significant is the corresponding coefficient [44]. So, it also implies that the variable with the largest effect was the initial nickel concentration for the percentage of nickel removal with OTP. Moreover, all correlation coefficients (higher than 0.91) were very high showing good fitness of statistical model.

### 3.2. Column biosorption modeling

From the statistical optimization, it is observed that the optimum values to maximize the OTP biosorption capacity (7.849 mg/g) for flow rate, biosorbent mass, and initial Ni(II) concentration, were estimated to be 8 mL/min, 5 g, and 100 mg/L; while to maximize the % of nickel removal (100%), were estimated to be 6 mL/min, 15 g, and 10 mg/L. For PCS, the optimum values to maximize the biosorption capacity (6.530 mg/g) were estimated to be 6 mL/min, 15 g,

Table 3  
Constant values for the fitted model of two responses for OTP

Biosorbent		Constant	Estimation	Standard error	p-Value
OTP	$Y_1 q_e$	$a_0$	67.9322	2.6029	
		$a_1$	-13.4444	2.4099	0.0000
		$a_2$	26.7033	2.4099	0.0000
		$a_3$	-50.1656	2.4099	0.0000
		$a_4$	-5.0867	4.1740	0.2396
		$a_5$	3.4167	2.9515	0.2630
		$a_6$	0.7650	2.9515	0.7986
		$a_7$	-13.7833	4.1740	0.0042
		$a_8$	6.31333	2.9515	0.0472
		$a_9$	8.7967	4.1740	0.0502
	$R^2 = 97.2889$ (percent); $R^2$ (adjusted for d.f.) = 95.8536 (percent); Standard error of Est = 5.1121				
	$Y_2\%$	$a_0$	5.4411	0.3389	
		$a_1$	1.6762	0.3138	0.0001
		$a_2$	-1.0629	0.3138	0.0035
		$a_3$	4.9269	0.3138	0.0000
		$a_4$	-0.6980	0.5435	0.2163
		$a_5$	0.3893	0.3843	0.3252
		$a_6$	0.9338	0.3843	0.0265
		$a_7$	0.59267	0.5435	0.2907
$a_8$		0.6592	0.3843	0.1045	
$a_9$		-2.6307	0.5435	0.0002	
$R^2 = 94.9950$ (percent); $R^2$ (adjusted for d.f.) = 92.3453 (percent); Standard error of Est = 0.6657					

and 100 mg/L and to maximize the % of nickel removal (100%) were estimated to be 6 mL/min, 15 g, and 10 mg/L.

Figs. 8 and 9 show the breakthrough curves with the optimum values for biosorption capacity and percentage of nickel removal onto OTP and PCS.

By analyzing Figs. 8 and 9, it is observed, as it is expected, that the results that make optimum value of the percentage of nickel removal (100%) for OTP and PCS, correspond to the experiments in which the time of contact coincides practically with the breakthrough time.

When the time of operation increases, the quantity of metal that is adsorbed in relation to the total quantity of metal that goes through the column decreases significantly, as well as the percentage of nickel adsorbed by the biosorbent.

On the other hand, the results that make optimum the biosorption capacity, correspond to the experiments in which the time of contact coincides practically with the saturation time.

In addition, figures show that the biosorbent OTP has reached the saturation, meanwhile the PCS has reached a value of  $C/C_i$  close to 0.8.

Therefore, only a model for the breakthrough curves could be obtained corresponding to the optimum values of biosorption capacity. The results for every model are shown below.

### 3.2.1. Adams–Bohart model

The Adams–Bohart adsorption model was applied to experimental data for the description of the initial part of the breakthrough curve. Parameter values for Adams–Bohart model were calculated using non-linear regression analysis according to Eq. (7) and presented in Table 6, together with the correlation coefficients and SS. The model does not reproduce the breakthrough curves adequately (see  $r^2$  values). However, the values of the maximum volumetric sorption,  $N_0$ , are higher for OTP, which agrees with that obtained experimentally.

Table 4  
Constant values for the fitted model of two responses for PCS

Biosorbent		Constant	Estimation	Standard error	P-Value
PCS	$Y_1 q_e$	$a_0$	60.2200	4.6289	
		$a_1$	-15.3678	4.2856	0.0023
		$a_2$	35.3722	4.2856	0.0000
		$a_3$	-55.7900	4.2856	0.0000
		$a_4$	-11.8967	7.4228	0.1274
		$a_5$	-8.8583	5.2487	0.1097
		$a_6$	-4.5667	5.2487	0.3964
		$a_7$	-9.4367	7.4228	0.2207
		$a_8$	14.4617	5.2487	0.0135
		$a_9$	26.0633	7.4228	0.0027
	$R^2 = 94.2405$ (percent); $R^2$ (adjusted for d.f.) = 91.1914 (percent); Standard error of Est = 9.0910				
	$Y_2\%$	$a_0$	4.9515	0.3605	
		$a_1$	1.1908	0.3338	0.0024
		$a_2$	-0.3063	0.3338	0.3716
		$a_3$	3.8371	0.3338	0.0000
		$a_4$	-1.7361	0.5781	0.0080
		$a_5$	-0.7655	0.4088	0.0784
		$a_6$	0.0470	0.4088	0.9098
		$a_7$	-0.6094	0.5781	0.3065
$a_8$		1.3147	0.4088	0.0051	
$a_9$		-1.0698	0.5781	0.0817	
$R^2 = 91.0602$ (percent); $R^2$ (adjusted for d.f.) = 86.3274 (percent); Standard error of Est = 0.7080					

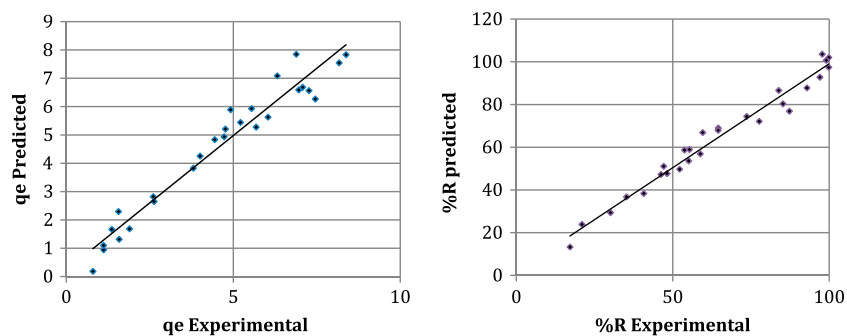


Fig. 6. Scatter graph of the predicted response values vs. experimental response value for the biosorption capacity of Ni(II) and nickel removal (%R) onto OTP.

### 3.2.2. Thomas model

The column data were fitted with the Thomas model to determine the Thomas rate constant ( $k_{Th}$ ) and maximum solid-phase concentration ( $q_0$ ). These parameters were obtained using non-linear regression analysis according to Eq. (8) and the results are listed in

Table 6. The Thomas model adequately reproduces the experimental data, obtaining  $r^2 > 0.95$ . However, the value obtained for the maximum solid-phase concentration for OTP (4.812 mg/g) is smaller than the experimental value (6.885 mg/g) and smaller than the value obtained from the statistical optimization (7.849 mg/g).

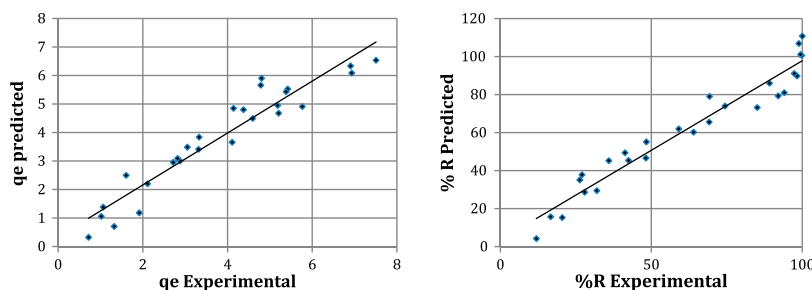


Fig. 7. Scatter graph of the predicted response values vs. experimental response value for the biosorption capacity of Ni(II) and nickel removal (%R) onto PCS.

Table 5  
Analysis of Variance (ANOVA) for OTP and PCS and for the two studied responses

Factor	OTP									
	$Y_1, q_e$					$Y_2, \%R$				
	SS	Df	MS	F-R	P-V	SS	Df	MS	F-R	P-V
A:Q	12.644	1	12.6437	28.53	0.0001	813.389	1	813.3890	31.12	0.0000
B:m	5.084	1	5.0838	11.47	0.0035	3208.810	1	3208.8100	122.78	0.0000
C:Ci	109.234	1	109.2340	246.52	0.0000	11324.600	1	11324.6000	433.33	0.0000
AA	0.731	1	0.7308	1.65	0.2163	38.811	1	38.8113	1.49	0.2396
AB	0.455	1	0.4547	1.03	0.3252	35.021	1	35.0208	1.34	0.2630
AC	2.616	1	2.6161	5.90	0.0265	1.756	1	1.7557	0.07	0.7986
BB	0.527	1	0.5269	1.19	0.2907	284.970	1	284.9700	10.90	0.0042
BC	1.303	1	1.3035	2.94	0.1045	119.575	1	119.5750	4.58	0.0472
CC	10.381	1	10.3806	23.43	0.0002	116.072	1	116.0720	4.44	0.0502
Total error	7.533	17	0.4431			444.274	17	26.1337		
Total (corr.)	150.507	26				16387.300	26			
	PCS									
A:Q	6.381	1	6.3808	12.73	0.0024	1062.760	1	1062.7600	12.86	0.0023
B:m	0.422	1	0.4223	0.84	0.3716	5630.370	1	5630.3700	68.13	0.0000
C:Ci	66.255	1	66.2554	132.17	0.0000	14006.400	1	14006.4000	169.47	0.0000
AA	4.521	1	4.5211	9.02	0.0080	212.296	1	212.2960	2.57	0.1274
AB	1.758	1	1.7580	3.51	0.0784	235.410	1	235.4100	2.85	0.1097
AC	0.007	1	0.0066	0.01	0.9098	62.563	1	62.5633	0.76	0.3964
BB	0.557	1	0.5571	1.11	0.3065	133.576	1	133.5760	1.62	0.2207
BC	5.185	1	5.1850	10.34	0.0051	627.419	1	627.4190	7.59	0.0135
CC	1.717	1	1.7166	3.42	0.0817	1018.950	1	1018.9500	12.33	0.0027
Total error	8.522	17	0.5013			1405.000	17	82.6471		
Total (corr.)	95.325	26				24394.700	26			

In contrast, the experimental and calculated values for the PCS are more similar (7.005, 7.505, and 6.530 mg/g), although the value obtained with Thomas model continues to be slightly smaller.

The difference in the value of the maximum biosorption capacity can be explained if it is considered that the Thomas model as well as the other models that have been used, take into account that the breakthrough curve is symmetric.

As it can be observed in the Figs. 8 and 9, the curves obtained are not symmetric, principally in the case of the OTP.

Thus, the time, when  $C/C_i = 0.5$  for OTP, is 30 min, meanwhile, the time to reach saturation (when  $C/C_i = 0.9$ ) is 100 min.

In the case of PCS, the curve presents a certain symmetry and even the saturation has not been reached, the time when  $C/C_i = 0.5$  is 170 min. The

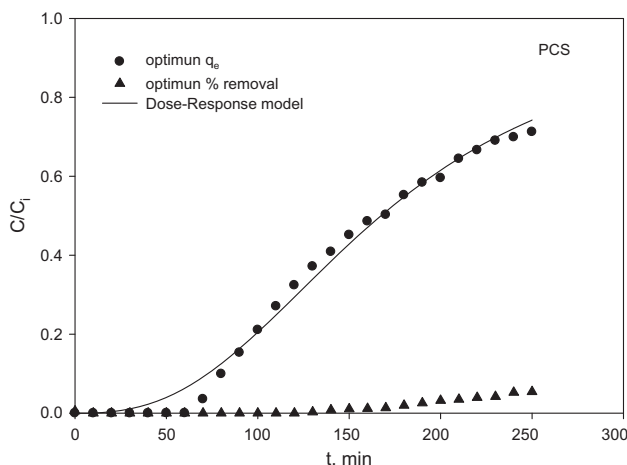
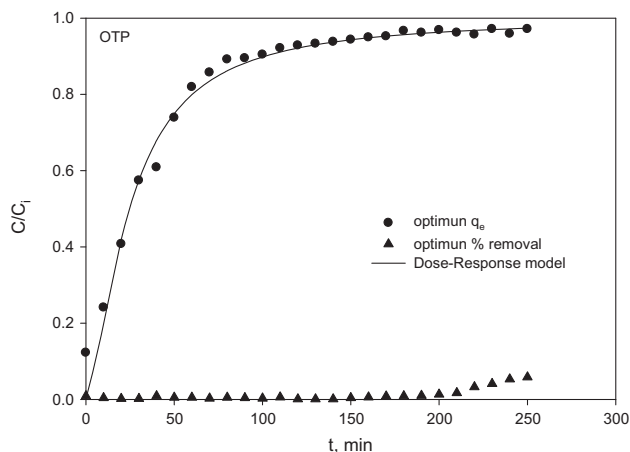


Fig. 8. Breakthrough curves with the optimum values for the biosorption capacity and the percentage of nickel removal onto OTP.

Fig. 9. Breakthrough curves with the optimum values for the biosorption capacity and the percentage of nickel removal onto PCS.

Table 6

Estimated parameter values for Adams–Bohart, Thomas, Yoon–Nelson, and Dose-response models for the biosorption process of Ni(II) onto OTP and PCS

Adams–Bohart model					
	$k_{AB}$ , L/mg min	$N_0$ , mg/L	$r^2$	$\sum \left[ \left( \frac{C}{C_i} \right)_{exp} - \left( \frac{C}{C_i} \right)_{cal} \right]^2$	
OTP	0.000197	4296.3	0.684	0.0376	
PCS	0.000175	3013.3	0.909	0.0582	
Thomas model					
	$k_{Th}$ , mL/mg min	$q_0$ , mg/g	$r^2$	$\sum \left[ \left( \frac{C}{C_i} \right)_{exp} - \left( \frac{C}{C_i} \right)_{cal} \right]^2$	
OTP	0.456	4.812	0.968	0.0503	
PCS	0.187	7.005	0.954	0.0852	
Yoon–Nelson model					
	$k_{YN}$ , min <sup>-1</sup>	$\tau_{cal}$ , min	$\tau_{exp}$ , min	$r^2$	$\sum \left[ \left( \frac{C}{C_i} \right)_{exp} - \left( \frac{C}{C_i} \right)_{cal} \right]^2$
OTP	0.0456	30.07	30.0	0.968	0.0503
PCS	0.0187	175.1	170.0	0.954	0.0852
Dose-response model					
	$a$	$q_0$ , mg/g	$r^2$	$\sum \left[ \left( \frac{C}{C_i} \right)_{exp} - \left( \frac{C}{C_i} \right)_{cal} \right]^2$	
OTP	1.711	4.554	0.982	0.0249	
PCS	2.636	6.693	0.991	0.0157	

saturation could be reached in 340 min as it can be deduced from the trend of the breakthrough curve.

This effect also happens if it  $q_e$  is calculated experimentally with the model when  $C/C_i = 0.5$ . The

values obtained in this way for OTP are 3.270 and 3.984 mg/g, respectively. That indicates that if the curve was symmetric, the results would be practically equal.

### 3.2.3. Yoon and Nelson model

The Yoon–Nelson model parameters can be obtained using non-linear regressive analysis from Eq. (9). The values of  $k_{YN}$  and  $\tau$  are listed in Table 6. The Yoon–Nelson is mathematically equal to Thomas model. So, Yoon–Nelson model reproduces adequately the experimental data, obtaining  $r^2$  values higher than 0.95. The 50% breakthrough time and  $\tau$  values are consistent to those obtained experimentally.

### 3.2.4. Dose-Response model

The model parameters were obtained using non-linear regression analysis according to Eq. (10) and the results are listed in Table 6. The predicted breakthrough curves of the Dose-Response model show reasonably good agreement with the experimental plots ( $r^2 > 0.98$ ) (see Figs. 8 and 9). The values of the maximum concentration of the solute in the solid phase,  $q_0$ , are similar to those obtained from Thomas model.

Once again, in the case of OTP, the model reproduces adequately the breakthrough curve. The value of maximum biosorption capacity obtained is smaller than the experimental one. For that, the model is more appropriate for curves which show symmetry.

Comparing all the models that have been used, it can be concluded that the Dose-Response model is the one that best reproduced the total breakthrough curves.

Although there are not similar studies to biosorption of Ni(II) in a packed bed column, obtained results were compared with the results obtained in previous studies with other metals [28,30,38]. In most cases, the Dose-Response model was the best model to adjust results and it minimized the errors resulting, especially in high values of operating time of the column.

## 4. Conclusions

Removal of nickel from aqueous solutions by biosorption onto two agro-industrial wastes in packed-bed columns was tested. Obtained results present contributions to science due to that they imply a new possible alternative to clean the industrial wastewater contaminated with nickel with a high efficiency. The significance of developing new treatment/removal methods for heavy metal from industrial wastewaters has been widely recognized especially in the fields of environmental sciences.

Concretely, in this work, the effects of operational parameters on biosorption capacity were studied and the breakthrough curves show that the percentage of nickel removal as well as the breakthrough time

increase, when the flow rate decreases, the mass of biosorbent is bigger and the initial concentration of Ni(II) is smaller.

Optimum biosorption conditions were determined by using a FFD, obtaining a high correlation between the experimental and predicted values ( $R^2 \approx 91\%$ ) that show good fitting of the models for the two responses analyzed (biosorption capacity and percentage of nickel removal) for both biosorbents. The best fitting is achieved using OTP as biosorbent with  $R^2 = 95\%$ .

The optimum flow rate, mass of biosorbent, and initial concentration of Ni(II) to obtain the maximum total nickel removal (100%) coincided for both biosorbents and were found to be 6 mL/min, 15 g, and 10 ppm. Meanwhile to maximize the biosorption capacity, the optimum flow rate, mass of biosorbent, and initial concentration of Ni(II), were 8 mL/min, 5 g, and 100 ppm for OTP and 6 mL/min, 15 g, and 100 ppm for PCS. Moreover, the optimum  $q_e$  obtained for OTP (7.849 mg/g) is greater than the optimum  $q_e$  obtained for PCS (6.530 mg/g).

The model equations obtained led to classify the parameters based on their level of significance for two responses analyzed. The optimization process concluded that the most influent parameter in biosorption capacity was initial concentration of Ni(II) followed by the flow rate, while the most influential factor in the percentage of nickel removal was the initial concentration of Ni(II) followed by the mass of biosorbent. It is also observed that all factors had higher influence over OTP than PCS.

Adams–Bohart, Thomas, Yoon–Nelson, and Dose-Response models were used to fit the experimental optimum data. Results showed that the Dose-Response model is the one that best reproduced the total breakthrough curves.

## References

- [1] B. Volesky, Z.R. Holan, Biosorption of heavy-metals, *Biotechnol. Progr.* 11 (1995) 235–250.
- [2] M. Sarkar, P. Majumdar, Application of response surface methodology for optimization of heavy metal biosorption using surfactant modified chitosan bead, *Chem. Eng. J.* 175 (2011) 376–387.
- [3] Nickel Institute. Knowledge for a brighter future, (accessed December 20, 2014). Available from: <<http://www.nickelinstitute.org>>.
- [4] Agency for Toxic Substances and Disease Registry. Nickel CAS ID#: 7440-02-0, (accessed January 12, 2015). Available from: <<http://www.atsdr.cdc.gov/substances/toxsubstance.asp?toxid=44>>.
- [5] M.N. Zafar, A. Parveen, R. Nadeem, A pretreated green biosorbent based on neem leaves biomass for the removal of lead from wastewater, *Desalin. Water Treat.* 51 (2013) 4459–4466.

- [6] C. Quintelas, Z. Rocha, B. Silva, B. Fonseca, H. Figueiredo, T. Tavares, Removal of Cd(II), Cr(VI), Fe (III) and Ni(II) from aqueous solutions by an *E. coli* biofilm supported on kaolin, *Chem. Eng. J.* 149 (2009) 319–324.
- [7] A. Ozturk, Removal of nickel from aqueous solution by the bacterium *Bacillus thuringiensis*, *J. Hazard. Mater.* 147 (2007) 518–523.
- [8] K. Vijayaraghavan, Y.S. Yun, Bacterial biosorbents and biosorption, *Biotechnol. Adv.* 26 (2008) 266–291.
- [9] Z. Reddad, C. Gearente, Y. Andreás, M.C. Ralet, J.F. Thibault, P. Le Cloirec, Ni(II) and Cu(II) binding properties of native and modified sugar beet pulp, *Carbohydr. Polym.* 49 (2002) 23–31.
- [10] V. Padmavathy, P. Vasudevan, S.C. Dhingra, Biosorption of nickel(II) ions on Baker's yeast, *Process Biochem.* 38 (2003) 1389–1395.
- [11] M.N. Zafar, R. Nadeem, M.A. Hanif, Biosorption of nickel from protonated rice bran, *J. Hazard. Mater.* 143 (2007) 478–485.
- [12] A. Ewecharoen, P. Thiravetyan, W. Nakbanpote, Comparison of nickel adsorption from electroplating rinse water by coir pith and modified coir pith, *Chem. Eng. J.* 137 (2008) 181–188.
- [13] K. Kishore, M. Xiaoguang, C. Christodoulatos, V.M. Boddu, Biosorption mechanism of nine different heavy metals onto biomatrix from rice husk, *J. Hazard. Mater.* 153 (2008) 1222–1234.
- [14] Y. Nuhoglu, E. Malkoc, Thermodynamic and kinetic studies for environmentally friendly Ni(II) biosorption using waste pomace of olive oil factory, *Bioresour. Technol.* 100 (2009) 2375–2380.
- [15] U. Farooq, J.A. Kozinski, M.A. Khan, M. Athar, Biosorption of heavy metal ions using wheat based biosorbents - A review of the recent literature, *Bioresour. Technol.* 101 (2010) 5043–5053.
- [16] A. Thevannan, R. Mungroo, C.H. Niu, Biosorption of nickel with barley straw, *Bioresour. Technol.* 101 (2010) 1776–1780.
- [17] H.R. Wu, C.I. Lin, L.H. Wang, Effect of peanut hull ash dosage on the degree of influence of operation variables of the adsorption of nickel ion from aqueous solution using peanut hull ash, *J. Taiwan Inst. Chem. Eng.* 42 (2011) 965–971.
- [18] I. Alomá, M.A. Martín-Lara, I.L. Rodríguez, G. Blázquez, M. Calero, Removal of nickel(II) ions from aqueous solutions by biosorption on sugarcane bagasse, *J. Taiwan Inst. Chem. Eng.* 43 (2012) 275–281.
- [19] T.A.H. Nguyen, H.H. Ngo, W.S. Guo, J. Zhang, S. Liang, Q.Y. Yue, Q. Li, T.V. Nguyen, Applicability of agricultural waste and by-products for adsorptive removal of heavy metals from wastewater, *Bioresour. Technol.* 148 (2013) 574–585.
- [20] M. El-Sadaawy, O. Abdelwahab, Adsorptive removal of nickel from aqueous solutions by activated carbons from doum seed (*Hyphaenethebaica*) coat, *Alexandria Eng. J.* 53 (2014) 399–408.
- [21] A.E. Ofomaja, E.B. Naidoo, S.J. Modise, Removal of copper(II) from aqueous solution by pine and base modified pine cone powder as biosorbent, *J. Hazard. Mater.* 168 (2009) 909–917.
- [22] A.E. Ofomaja, E.B. Naidoo, Biosorption of copper from aqueous solution by chemically activated pine cone: A kinetic study, *Chem. Eng. J.* 175 (2011) 260–270.
- [23] M. Calero, A. Pérez, G. Blázquez, A. Ronda, M.A. Martín-Lara, Characterization of chemically modified biosorbents from olive tree pruning for the biosorption of lead, *Ecol. Eng.* 58 (2013) 344–354.
- [24] M.Y. Can, Y. Kaya, O.F. Algur, Response surface optimization of the removal of nickel from aqueous solution by cone biomass of *Pinus sylvestris*, *Bioresour. Technol.* 97 (2006) 1761–1765.
- [25] M.A. Martín-Lara, I. Rodríguez, G. Blázquez, M. Calero, Factorial experimental design for optimizing the removal conditions of lead ions from aqueous solutions by three wastes of the olive-oil production, *Desalination* 278 (2011) 132–140.
- [26] D. Bingöl, M. Hecan, S. Eleveli, E. Kılıç, Comparison of the results of response surface methodology and artificial neural network for the biosorption of lead using black cumin, *Bioresour. Technol.* 112 (2012) 111–115.
- [27] M. Calero, A. Ronda, M.A. Martín-Lara, A. Pérez, G. Blázquez, Chemical activation of olive tree pruning to remove lead(II) in batch system: Factorial design for process optimization, *Biomass Bioenergy* 58 (2013) 322–332.
- [28] M. Calero de Hoces, G. Blázquez García, A. Gálvez, M.A. Martín-Lara, Effect of the Acid Treatment of Olive Stone on the Biosorption of Lead in a Packed-Bed Column, *Ind. Eng. Chem. Res.* 49 (2010) 12587–12595.
- [29] G.E.P. Box, W.G. Hunter, J.S. Hunter, *Statistics for Experimenters: An Introduction to Design, Data Analysis, and Model Building*, Wiley, New York, NY, 1978.
- [30] M. Calero, F. Hernáinz, G. Blázquez, G. Tenorio, M.A. Martín-Lara, Study of Cr(III) biosorption in a fixed-bed column, *J. Hazard. Mater.* 171 (2009) 886–893.
- [31] M.A. Martín-Lara, F. Hernáinz, G. Blázquez, G. Tenorio, M. Calero, Sorption of Cr(VI) onto olive stone in a packed bed column: prediction of kinetic parameters and breakthrough curves, *J. Environ. Eng.* 136 (2010) 1389–1397.
- [32] A.R. Khataee, M. Zarei, S.K. Asl, M. Dachraoui, M.A. Oturan, Photocatalytic treatment of a dye solution using immobilized TiO<sub>2</sub> nanoparticles combined with photoelectro-Fenton process: Optimization of operational parameters, *J. Electroanal. Chem.* 648 (2010) 143–150.
- [33] R. Han, J. Zhang, W. Zou, H. Xiao, J. Shi, H. Liu, Biosorption of copper(II) and lead(II) from aqueous solution by chaff in a fixed-bed column, *J. Hazard. Mater.* 133 (2006) 262–268.
- [34] S.H. Hasan, P. Srivastava, D. Ranjan, M. Talat, Biosorption of Cr(VI) from aqueous solution using *A. hydrophila* in up-flow column: optimization of process variables, *Appl. Microbiol. Biotechnol.* 83 (2009) 567–577.
- [35] U. Farooq, M. Athar, M.A. Khan, J.A. Kozinski, Biosorption of Pb(II) and Cr(III) from aqueous solutions: breakthrough curves and modeling studies, *Environ. Monit. Assess.* 185 (2013) 845–854.
- [36] R. Han, Y. Wang, W. Yu, W. Zou, J. Shi, H. Liu, Biosorption of methylene blue from aqueous solution by rice husk in a fixed-bed column, *J. Hazard. Mater.* 141 (2007) 713–718.

- [37] A. Singh, D. Kumar, J.P. Gaur, Continuous metal removal from solution and industrial effluents using *Spirogyra* biomass-packed column reactor, *Water Res.* 46 (2012) 779–788.
- [38] M. Calero de Hoces, G. Blázquez García, A. Ronda Gálvez, A.E. Álvarez, M.A. Martín-Lara, Biosorption of  $\text{Cu}^{2+}$  in a packed bed column by almond shell: Optimization of process variables, *Desalin. Water Treat.* 51 (2013) 1954–1965.
- [39] E. Oguz, M. Ersoy, Biosorption of cobalt(II) with sunflower biomass from aqueous solutions in a fixed bed column and neural networks modelling, *Ecotoxicol. Environ. Saf.* 99 (2014) 54–60.
- [40] V. Ponnusami, V. Krithika, R. Madhuram, S.N. Srivastava, Biosorption of reactive dye using acid-treated rice husk: Factorial design analysis, *J. Hazard. Mater.* 142 (2007) 397–403.
- [41] J. Liu, M. Yan, Y.K. Zhang, K.F. Du, Study of glutamate-modified cellulose beads for Cr(III) adsorption by response surface methodology, *Ind. Eng. Chem. Res.* 50 (2011) 10784–10791.
- [42] S.H. Hasan, P. Srivastava, M. Talat, Biosorption of lead using immobilized *Aeromonas hydrophila* biomass in up flow column system: Factorial design for process optimization, *J. Hazard. Mater.* 177 (2010) 312–322.
- [43] T. Ölmez, The optimization of Cr(VI) reduction and removal by electrocoagulation using response surface methodology, *J. Hazard. Mater.* 162 (2009) 1371–1378.
- [44] A.I. Khuri, J.A. Cornell, *Response Surface: Design and Analysis*, Marcel Dekker, New York, NY, 1987.